

# Proportional Control for Stochastic Regulation on Allocation of Multi-Robots

Thales C. Silva, Victoria Edwards, and M. Ani Hsieh

University of Pennsylvania, Department of Mechanical Engineering and Applied  
Mechanics, Philadelphia, PA 19104, USA  
scthales@seas.upenn.edu

**Abstract.** Any strategy used to distribute a robot ensemble over a set of sequential tasks is subject to inaccuracy due to robot-level uncertainties and environmental influences on the robots’ behavior. We approach the problem of inaccuracy during task allocation by modeling and controlling the overall ensemble behavior. Our model represents the allocation problem as a stochastic jump process and we regulate the mean and variance of such a process. The main contributions of this paper are: Establishing a structure for the transition rates of the equivalent stochastic jump process and formally showing that this approach leads to decoupled parameters that allow us to adjust the first- and second-order moments of the ensemble distribution over tasks, which gives the flexibility to decrease the variance in the desired final distribution. This allows us to directly shape the impact of uncertainties on the group allocation over tasks. We introduce a detailed procedure to design the gains to achieve the desired mean and show how the additional parameters impact the covariance matrix, which is directly associated with the degree of task allocation precision. Our simulation and experimental results illustrate the successful control of several robot ensembles during task allocation.

**Keywords:** multi-robot system, control, task-allocation

## 1 Introduction

Modeling an ensemble of robots as an aggregate dynamical system offers flexibility in the task assignment and is an alternative to traditional bottom-up task allocation methods, which usually are computationally expensive (see [3,5] and references therein). Given a desired allocation of robots to tasks, each robot must navigate, handle dynamic constraints, and interact with the environment to achieve the desired allocation while meeting some desired team-level performance specifications. It is well understood that uncertainties resulting from the robot’s interactions with the environment, execution of its assigned tasks, and noise from its own sensors and actuators might lead to several issues during task allocation (*e.g.*, performance loss and inaccuracy) [13,14]. This is because allocations are often computed prior to execution and do not account for uncertainties that arise during runtime. In addition, analysis of the team-level performance

of swarms has shown that local (and sometimes small) deviations from the required performance at the robot level can combine and propagate, leading to substantial changes in the behavior of the whole group, which might result in loss of performance for the entire team (see Section 2 in [7]). Consequently, addressing the fundamental question of how to properly represent and design robot ensemble behaviors to meet the desired performance requirements can help us to improve our understanding of such complex systems.

An existing category of ensemble models uses stochastic processes to represent robot teams [4,8,11]. These models use random variables to describe the population of robots performing tasks, whereas transitions between tasks are described based on jump processes with random arrival times. Using these representations it is possible to design stable equilibria that reflect desired distributions of the robots over tasks [1,2]. In addition, it is also possible to account for and to incorporate heterogeneous sensing and mobility capabilities in a robot team using these models [17,18]. One of the major advantages of these macroscopic representations is their ability to scale to larger team sizes since their complexity is solely a function of the number of tasks. In contrast, the complexity of traditional task allocation methods grows as the number of agents and tasks increases.

Nevertheless, most macroscopic approaches are accurate for an asymptotically large number of agents, *i.e.*, when  $N \rightarrow \infty$ , where  $N$  represents the number of robots in the team. Fundamentally, within this assumption is the notion that no individual robot’s deviations from its desired performance will greatly impact the team’s performance as a whole. And yet Tarapore *et al.*, [19] recently discussed the challenges associated with employing large teams of robots in real world applications. Considering the impracticability of dense swarms in several applications, they propose *sparse swarms* arguing that guiding the research toward low-density swarms is more relevant to real-world applications. One of the goals of this paper is to address the large number assumption by providing a method to regulate the variance of a robot distribution in the task allocation problem. Specifically, by explicitly controlling the mean of the robot distribution and independently controlling its variance we can employ our methodology in teams with a relatively small number of agents, that is, we decrease the impact of individual robot deviations on the team’s performance. Hence, our methodology is a stride towards accurately modeling the allocation dynamics of these *sparse swarms*. While similar techniques exist [12], the proposed strategy lacks the ability to simultaneously control both the first- and second-order moments. Instead, we leverage the work from Klavins [10], which considers a *stochastic hybrid system* to model and control the mean and variance of molecular species concentrations. We extend this result to robot swarm applications, which fundamentally alter some of the assumptions in [10], for example, in our setting we are concerned about teams of constant size without a set of continuous variables. In robotics, Napp *et al.*, [15] presented an integral set point regulation technique, employed to regulate the mean of the robot population performing specific tasks. While they highlighted the importance of considering variance control, since the

mean can be a sensitive control objective, they do not propose a methodology to adjust the variance.

In this paper, we present a strategy to govern the mean and variance of the distribution of robots across a set of tasks. The contributions of this work include 1) a decoupled formulation of the first- and second-order moments for an ensemble model of robot teams that allows their adjustment individually, and 2) systematic methods to determine the control gains to achieve the desired distributions of robots over tasks. Our experimental results indicate that our proposed macroscopic techniques allows for improved control of small number teams.

## 2 Problem formulation

### 2.1 Graph Theory

We are interested in the stochastic behavior of a robot ensemble generated by robot-level uncertainties. We assume a group of  $N \in \mathbb{N}$  robots executing  $M \in \mathbb{N}$  spatially distributed tasks, the relationship among tasks is represented by a graph  $\mathcal{G}(\mathcal{V}, \mathcal{E})$ , in which the elements of the node set  $\mathcal{V} = \{1, \dots, M\}$  represent the tasks, and the edge set  $\mathcal{E} \subset \mathcal{V} \times \mathcal{V}$  maps adjacent allowable switching between task locations. Each element of the edge set represents a directed path from  $i$  to  $j$  if  $(i, j) \in \mathcal{E}$ . A graph  $\mathcal{G}$  is called an *undirected graph* if  $(i, j) \in \mathcal{E} \iff (j, i) \in \mathcal{E}$ . We define the neighborhood of the  $i$ th task node as the set formed by all tasks that have the  $i$ th task as a child node and it is denoted by  $\mathcal{N}_i = \{j \in \mathcal{V} : (j, i) \in \mathcal{E}\}$ . We call a neighbor of a task  $i$  an adjacent task  $j$  that belongs to  $\mathcal{N}_i$ . In this paper we assume the following:

**Assumption 1** *The graph that maps the relationship between tasks,  $\mathcal{G}(\mathcal{V}, \mathcal{E})$ , is connected and undirected.*

Assumption 1 allows the robots to sequentially move back and forth between tasks. For some task topologies, it is possible to adjust the transition parameters such that directionality in the task graph is obtained [2].

### 2.2 Ensemble Model

To derive the macroscopic ensemble model for the  $N$  robot team simultaneously executing  $M$  tasks, we assume each robot can execute only one task at a given time and it must switch between adjacent tasks to complete the team's wide objective. The model needs to capture the global stochastic characteristics that emerge from a robot's interaction with other robots and the environment, such as variations in terrain [17,12], collision avoidance [11], and delays [1]. Thus, the state of our system is given by a vector of random variables  $\mathbf{X}(t) = [X_1(t) \ \cdots \ X_M(t)]'$ , where the prime symbol in a vector,  $\mathbf{a}'$ , denotes its transpose, and each element of  $\mathbf{X}(t)$  describes the number of robots executing the respective task at time  $t$ , therefore  $\sum_{i=1}^M X_i(t) = N$  for any  $t \geq 0$ .

We aim to characterize the evolution of the random variable  $X_i(t)$ , for each  $i \in \{1, \dots, M\}$  and, ultimately, regulate its value. However, the stochastic nature of these variables might lead to convergence only to a vicinity of the desired value, where the size of the convergence region depends on robot-level deviations from the desired performance [9]. In principle, the control of systems subject to random variations could be approached by applying robust control techniques and defining input-to-state stability criteria. However, in our scenario, defining bounds for variations of robot-level behavior for a general number of tasks and robots can be difficult. Therefore, we approach the problem by controlling the mean value of the state variables  $X_i(t)$  and the dynamics of their second-order moments. Observe that the vicinity size of the desired objective is directly associated with the second-order moment.

The states of our system characterize pure jump processes  $X_i(t) : [0, \infty) \rightarrow \mathcal{D}$ , where  $\mathcal{D}$  is a finite discrete set. In particular, let  $\psi : \mathcal{D} \times [0, \infty) \rightarrow \mathbb{R}$  be a real-valued function, it is a known result that the dynamics of the expected value of  $\psi$  is described by the following relation (see Chapter 1 in [16]),

$$\frac{d}{dt}E[\psi(X_i(t))] = E[\mathcal{L}\psi(X_i(t))],$$

in which  $\mathcal{L}$  is the infinitesimal generator of the stochastic process defined as

$$\mathcal{L}\psi(X_i(t)) = \sum_{\ell} [\psi(\phi_{\ell}(X_i(t))) - \psi(X_i(t))] \lambda_{\ell}(X_i(t)), \quad (1)$$

where  $\lambda_{\ell}(X_i(t))$  is a function of the number of robots at task  $X_i$  and in its neighborhood which describes the rate of transitions, *i.e.*,  $\lambda_{\ell}(X_i(t))dt$  represents the probability of a transition in  $X_i(t)$  occurring in  $dt$  time,  $\phi_{\ell}(X_i(t))$  maps the size of a change on  $X_i(t)$  given that an  $\ell$  transition happened. In our case, we assume two possible unitary changes in  $dt$ , a transition of type  $\ell = 1$ , in which one agent leaves  $X_i(t)$  defined by  $\phi_1(X_i(t)) = X_i(t) - 1$ , and of type  $\ell = 2$  where one agent arrives  $X_i(t)$ , defined by  $\phi_2(X_i(t)) = X_i(t) + 1$ . Hence,  $\ell \in \{1, 2\}$  maps the type of transition, *i.e.*, one robot leaving or one agent arriving at  $X_i(t)$ , respectively.

In this paper, we are interested in enforcing desired first- and second-order moments of the distribution of robots across tasks. Specifically, the problem investigated can be stated as:

**Problem 1.** Given  $M$  tasks to be dynamically executed by  $N$  robots, in which the switching between adjacent tasks is represented by the topology of the task graph  $\mathcal{G}(\mathcal{V}, \mathcal{E})$ , define a feedback controller that changes the transition rates  $\lambda_{\ell}(X_i)$ , for all  $i \in \{1, \dots, M\}$ , such that the distribution of first- and second-order moments converge to the desired value.

It is important to note that a solution for a similar problem was previously proposed in [11,12]. Even though they were motivated by the study from Klavins



[10], the proposed control strategy relies on a feedback linearization action, which leads to a closed-loop system of the form (see equation (9) in [11])

$$\frac{d}{dt}E[X(t)] = (\mathbf{K}_\alpha + \mathbf{K}_\beta)E[X(t)],$$

where  $\mathbf{K}_\alpha$  is a matrix that maps the transition rate of the system and  $\mathbf{K}_\beta$  is a matrix with new parameters to attain the desired variance. The main drawback of this approach is twofold: i) by changing  $\mathbf{K}_\beta$  the stationary distribution of the equivalent Markov chain also changes, which makes it necessary to readjust the gains for the whole system, and ii) addressing the regulation of second-order moments using  $\mathbf{K}_\beta$  is *equivalent* to changing the transition rate of the whole process during the entire evolution. In comparison, our proposed strategy overcomes these limitations by simply manipulating the graph structure and defining a new structure for  $\lambda_\ell(\cdot)$ , in such a way that the new feedback strategy does not directly modify the stationary distribution of the equivalent Markov chain and provides changes to the transition rates according to the current state of the system. We describe our methodology in the following section.

### 3 Methodology

#### 3.1 Control Strategy

We model the arrival and departure of robots by pure stochastic jump processes. For example, for two tasks:

$$X_1(t) \xleftrightarrow[\lambda(\cdot)]{} X_2(t) \quad (2)$$

the random variables  $X_1(t)$  and  $X_2(t)$  represent the number of robots in each task at time  $t$ , and  $\lambda_\ell(X_i)$  for  $\ell \in \{1, 2\}$  maps the transition rate of agents between tasks. Motivated by Klavins [10] on gene regulatory networks, we approach Problem 1 by defining the transition rate functions with a term that is proportional with the number of agents on a given site and in its neighborhood. In equation (2) this choice means that switching from task 1 to 2 and from 2 to 1 will depend on the number of agents at both tasks. In particular, for equation (1) we define the transition rates as,

$$\lambda_1(X_i) = \sum_{j \in \mathcal{N}_i} k_{ij}X_i - \beta_i X_i X_j, \quad (3)$$

$$\lambda_2(X_i) = \sum_{j \in \mathcal{N}_i} k_{ji}X_j - \beta_i X_i X_j. \quad (4)$$

*Remark 1.* A necessary condition for the equations in (3) and (4) to be valid transition rates is being non-negative. While it is possible to guarantee positiveness during the whole evolution for some well-designed initial conditions with careful choices of gains, we instead, let robots transition back to previous tasks

before the team reaches steady-state by mapping the equivalent non-negative transition with reversed direction. This flexibility is the justification for Assumption 1.

It is worth noticing that our control strategy is distinct from the one presented in [10]. Here, we only require the transition rate to be adjusted according to the current number of agents in the tasks and in their neighborhood. While in [10] it is assumed that each node in the network has a *source* and a *sink*, which implies that the variation on the value of the random variable  $X_i$  can increase or decrease independently of the variation in its neighbors, in addition to the switching between adjacent nodes.

In the following, we show that with our choice for the transition rates  $\lambda_\ell(X_i)$ , the first-order moment depends only on the parameter  $k_{ij}$ , while the variable  $\beta_i$  manifests on the second-order moments. This introduces a free variable, allowing the variance to be properly adjusted.

Defining  $\psi(X_i) = X_i$  and applying the infinitesimal generator (1) with the transition rates in (3) and (4), we get the following first-order moment for a general arrangement,

$$\begin{aligned} \frac{d}{dt}E[X_i] &= E \left[ \sum_{j \in \mathcal{N}_i} (k_{ji}X_j - \beta_i X_i X_j) - \sum_{j \in \mathcal{N}_i} (k_{ij}X_i - \beta_i X_j X_i) \right] \\ &= \sum_{j \in \mathcal{N}_i} (k_{ji}E[X_j] - k_{ij}E[X_i]). \end{aligned}$$

While for the second-order moments we define  $\psi(X_i) = X_i^2$ ,

$$\begin{aligned} \frac{d}{dt}E[X_i^2] &= E \left[ ((X_i + 1)^2 - X_i^2) \sum_{j \in \mathcal{N}_i} (k_{ji}X_j - \beta_i X_i X_j) \right. \\ &\quad \left. + ((X_i - 1)^2 - X_i^2) \sum_{j \in \mathcal{N}_i} (k_{ij}X_i - \beta_i X_j X_i) \right] \\ &= E \left[ \sum_{j \in \mathcal{N}_i} (2k_{ji}X_i X_j - 2k_{ij}X_i X_i + k_{ij}X_i + k_{ji}X_j - 2\beta_i X_i X_j) \right], \end{aligned}$$

and for off-diagonal terms,

$$\begin{aligned}
\frac{d}{dt}E[X_i X_q] &= E \left[ ((X_i + 1)X_q - X_i X_q) \sum_{j \in \mathcal{N}_i} (k_{ji} X_j - \beta_i X_i X_j) \right. \\
&\quad + ((X_q + 1)X_i - X_i X_q) \sum_{j \in \mathcal{N}_q} (k_{jq} X_j - \beta_q X_q X_j) \\
&\quad + ((X_i - 1)X_q - X_i X_q) \sum_{j \in \mathcal{N}_i} (k_{ij} X_i - \beta_i X_i X_j) \\
&\quad \left. + ((X_q - 1)X_i - X_i X_q) \sum_{j \in \mathcal{N}_q} (k_{qj} X_q - \beta_q X_q X_j) \right] \\
&= E \left[ \sum_{j \in \mathcal{N}_i} (k_{ji} X_q X_j - k_{ij} X_i X_q) + \sum_{j \in \mathcal{N}_q} (k_{jq} X_i X_j - k_{qj} X_q X_i) \right].
\end{aligned}$$

An important property of these equations is that they are in closed-form, which allows us to use them to design gains to attain the desired distribution. For a compact vectorized form, let  $\mathbf{K}$  be an  $M \times M$  matrix defined as follows,

$$\mathbf{K}_{ij} = \begin{cases} k_{ij} & \text{if } (j, i) \in \mathcal{E}, \\ -\sum_q k_{iq} & \text{if } i = j, \\ 0 & \text{otherwise,} \end{cases} \quad (5)$$

then the first- and second-order moments can be written as,

$$\frac{d}{dt}E[\mathbf{X}] = \mathbf{K}E[\mathbf{X}], \quad (6)$$

$$\begin{aligned}
\frac{d}{dt}E[\mathbf{X}\mathbf{X}'] &= \mathbf{K}E[\mathbf{X}\mathbf{X}'] + E[\mathbf{X}\mathbf{X}']\mathbf{K}' \\
&\quad + \sum_{i=1}^M e_i e_i' \otimes \left( \sum_{j \in \mathcal{N}_i} (k_{ij} E[X_i] + k_{ji} E[X_j] - 2\beta_i E[X_i X_j]) \right), \quad (7)
\end{aligned}$$

where  $e_i$ , for  $i = 1, \dots, M$ , are the canonical basis of  $\mathbb{R}^M$  and  $\otimes$  denotes the Kronecker product. Equations (6) and (7) model the dynamics of the first- and second-order moments of a group of  $N$  robots executing  $M$  tasks. There are two important underlying assumptions on this representation, first we assume the timing for robots to leave and arrive at a task follows a Poisson process. We believe this assumption is not too restrictive since, as discussed above, robot level deviations from desired performance will impact the scheduling, leading to stochastic jump processes. The second assumption, and arguably the hardest to justify for general systems, is that *we can actuate on the system's transition rates*. To be able to do this in our case, notice the structure of  $\lambda_\ell(\cdot)$  in (3) and (4), we need to monitor the current number of agents at each task and their neighborhood and then communicate this value to each agent at these

sites to compute the switching time. Dynamically defining the transition rates has an intricate relationship with the allocated time and microscopic deviations. We expect that the feedback nature of our approach accounts for microscopic deviations from the desired performance in the long run.

### 3.2 Control Analysis

In this section we analyse the convergence of the mean to the desired distribution and show a simple method to obtain the parameters of the gain matrix  $\mathbf{K}$ .

**Theorem 1.** *Let  $N$  agents execute  $M$  tasks organized according to an undirected graph  $\mathcal{G}(\mathcal{V}, \mathcal{E})$ . Given a desired stationary distribution  $E[\mathbf{X}^d]$  such that  $\sum_{i=1}^M X_i^d = N$ , the robot ensemble converges asymptotically to  $E[\mathbf{X}^d]$  from any initial distribution, with transition rates defined in (3) and (4), if, and only if  $\mathbf{K}E[\mathbf{X}^d] = \mathbf{0}$ .*

*Proof.* The demonstration follows from standard Lyapunov analysis. Note that, by definition, the eigenvalues of matrix  $\mathbf{K}$  have negative real part, except for one which is zero, that is,  $0 = \sigma_1(\mathbf{K}) > \sigma_2(\mathbf{K}) \geq \dots \geq \sigma_M(\mathbf{K})$ , where  $\sigma_i(\mathbf{K})$  denotes the  $i$ th eigenvalue of  $\mathbf{K}$ . Hence, defining a simple Lyapunov function candidate,  $V = E[\mathbf{X}]'PE[\mathbf{X}]$ , where  $P$  is a symmetric positive definite matrix. The time-derivative of  $V$  along the trajectories of the first-order moments yields

$$\frac{dV}{dt} = E[\mathbf{X}]'(\mathbf{K}'P + P\mathbf{K})E[\mathbf{X}],$$

because every eigenvalue of  $\mathbf{K}$  has negative or zero real part, we have that

$$\frac{dV}{dt} \leq 0.$$

Consider the invariant set  $S = \{E[\mathbf{X}] \in \mathbb{R}^M : \frac{dV}{dt} = 0\}$ , since the robots will always be in one of the graph's nodes, *i.e.*,  $\sum_{i=1}^M X_i = N$ , we have that  $E[\mathbf{X}(t)] \neq \mathbf{0}$  for all  $t > 0$ . Therefore, no solution can stay in  $S$  other than  $E[\mathbf{X}^d]$ , in other words, the equilibrium point  $E[\mathbf{X}^d]$  is globally asymptotically stable.

Notice that we assumed that each robot will always be assigned to one task at any instant, to consider robots in transit between nodes it is possible to extend the task graph as in [1]. In addition, by construction,  $\mathbf{K}$  results in a stable ensemble. The compelling aspect of Theorem 1 with respect to our model for the first- and second-order moment, equations (6) and (7), is that we can use the condition provided on the theorem to design the gains to attain a desired distribution, while still having free variables  $\beta_i$  to adjust the second-order terms. We compute the gain matrix  $\mathbf{K}$  by solving the following optimization:

$$\begin{aligned} \mathbf{K} &= \underset{\mathbf{Q}}{\operatorname{argmin}} \|\mathbf{Q}E[\mathbf{X}^d]\| \\ \text{s.t. } \mathbf{1}'\mathbf{Q} &= \mathbf{0}; \mathbf{Q} \in \mathcal{K}; \text{ structure in (5),} \end{aligned} \tag{8}$$

where the set  $\mathcal{K}$  accounts for the set of possible rate matrices for a given set of tasks and  $E[\mathbf{X}^d] \in \text{Null}(\mathbf{Q})$  is the desired final distribution.

At the moment, although we have shown additional tuning variables in our approach, we do not have a methodology to compute appropriate gains  $\beta_i$  for a desired covariance matrix. Nonetheless, we give an intuition of the mechanism of how they impact the steady-state covariance matrix. Let  $\mathbf{C} = E[(\mathbf{X} - E[\mathbf{X}])(\mathbf{X} - E[\mathbf{X}])']$  be the covariance matrix, replacing  $E[\mathbf{X}\mathbf{X}']$  in (7) and recalling that  $\mathbf{K}E[\mathbf{X}] = \mathbf{0}$  during the steady-state, analysing the equilibrium point  $\frac{d}{dt}E[\mathbf{X}\mathbf{X}'] = \mathbf{0}$  gives us

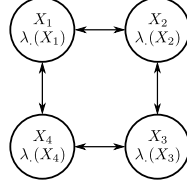
$$\mathbf{K}\mathbf{C} + \mathbf{C}\mathbf{K}' = - \sum_{i=1}^M e_i e_i' \otimes \left( \sum_{j \in \mathcal{N}_i} (k_{ij} E[X_i^d] + k_{ji} E[X_j^d] - 2\beta_i E[X_i^d X_j^d]) \right).$$

Since every eigenvalue of  $\mathbf{K}$  has negative real part except for one which is equal to zero, and  $E[\mathbf{X}^d] \neq \mathbf{0}$ , we have an unique solution for  $\mathbf{C}$  [9,10]. Therefore, the additional tuning variables  $\beta_i$ , for  $i \in \mathcal{V}$  are inversely proportional to the covariance at the steady-state—the bigger the values of  $\beta_i$ , while (3) and (4) are positive during the steady-state (recalling Remark 1), the smaller the covariance.

## 4 Results

### 4.1 Numerical Simulations

*Example 1.* We use the stochastic simulation algorithm proposed by Gillespie [6] to evaluate the proposed control strategy. We present a four task example,  $M = 4$ , with the topology represented in Figure 1 (a). We run two different tests to evaluate the effectiveness of our method, one with parameters  $\beta_i = 0$ , for  $i = 1, \dots, 4$ , and another with nonzero  $\beta_i$  parameters (values given below). In both cases, we aim to achieve the same final distribution. The initial populations at each task is given by  $\mathbf{X}_0 = [5 \ 15 \ 5 \ 5]'$ , and the desired distribution is  $E[\mathbf{X}^d] = [13 \ 9 \ 6 \ 2]'$ . The gain matrix  $\mathbf{K}$  used to reach such a distribution was computed solving the optimization problem (8) with  $\mathcal{K} = \{\mathbf{K} \in \mathbb{R}^{4 \times 4} : \mathbf{K} \leq -1.5\mathbf{I}\}$ , this constraint was imposed to ensure not too long convergence time. The resulting parameters from the optimization are  $k_{12} = 2.1$ ,  $k_{14} = 1.4$ ,  $k_{21} = 1.5$ ,  $k_{23} = 1.3$ ,  $k_{32} = 0.9$ ,  $k_{34} = 1.2$ ,  $k_{41} = 0.1$ ,  $k_{43} = 0.6$ , and 0 elsewhere outside the main-diagonal. We computed the mean and variance from the simulation considering 130 data points sampled for  $t > 2.0$  seconds in each simulation. This number was chosen to match the sample size between the two experiments. The simulation with  $\beta_i = 0$  for all  $i = 1, \dots, 4$  in Figure 1 (b) has the following mean  $E[\mathbf{X}] = [12.16 \ 9.76 \ 5.18 \ 2.77]'$ , and variances,  $\text{diag}(E[\mathbf{X}\mathbf{X}']) = [5.78 \ 6.83 \ 4.20 \ 1.44]'$ . The variances were improved by greedily modifying  $\beta_i$  values—if the variance was reduced and did not actively disturb another task population variance then that value was kept. Figure 1 (c) used parameters  $\beta_1 = 0.05$ ,  $\beta_2 = 0.20$ ,  $\beta_3 = 0.11$ , and  $\beta_4 = 0.052$ , where the resulting means are  $E[\mathbf{X}] = [12.26 \ 9.30 \ 5.83 \ 2.60]'$  variances are  $\text{diag}(E[\mathbf{X}\mathbf{X}']) = [1.06 \ 1.12 \ 1.15 \ 0.45]'$ .



(a) Graph Topology

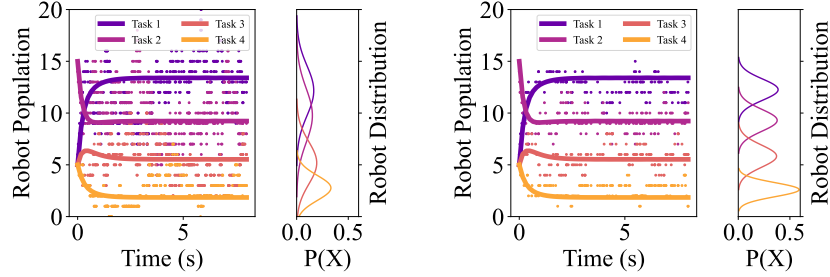
(b) Realization with  $\beta_i = 0, \forall i \in \mathcal{V}$ (c) Realization with  $\beta_i \neq 0, \forall i \in \mathcal{V}$ 

Fig. 1: The graph topology is depicted in (a). In (b) and (c) it is shown a realization of each of the stochastic simulations, where the dots represent the number of agents and the solid lines represent the numerical solution of (6). The tasks are identified by the color caption. The realization in (b) uses  $\beta_i = 0, \forall i \in \mathcal{V}$ , while in (c) is with  $\beta_1 = 0.05, \beta_2 = 0.20, \beta_3 = 0.11$ , and  $\beta_4 = 0.052$ .

These results highlight the impact of variability on small size teams ( $N = 30$ ). Visually, the control reduces the variance throughout the experiment, especially once steady-state is reached. It is worth mentioning that we have tested our strategy on larger teams and the results were in agreement with our hypothesis that it is possible to shape the variance using (3) and (4), however, due to space limitations of the venue, we chose to not show those results.

*Example 2.* In this example, we run 6 different trials with varying team sizes to numerically evaluate the variation in accuracy for teams of different sizes. To this end, we consider four tasks with topology represented in Figure 1 (a), and we computed the variance considering 160 data points sampled from each simulation for  $t > 2.0$  seconds. In addition, we vary the total number of robots between simulations, hence relative the initial and desired distributions for each simulation are:  $\mathbf{X}_0 = [25\% \ 25\% \ 0\% \ 50\%]'$ , and  $E[\mathbf{X}^d] = [50\% \ 50\% \ 0\% \ 0\%]'$ , respectively, given as a percentage of the total number of robots in the team. In these simulations, we used the same values for the parameters  $\beta_i$  as in Example 1, and we do not change them between simulations. To provide an intuition of the level of spread in each scenario, we compute the Relative Variance (RV) as the quotient of the mean by the variance of the respective task. The results are

presented in Table 1. We notice that for this scenario, the RV for the multi-

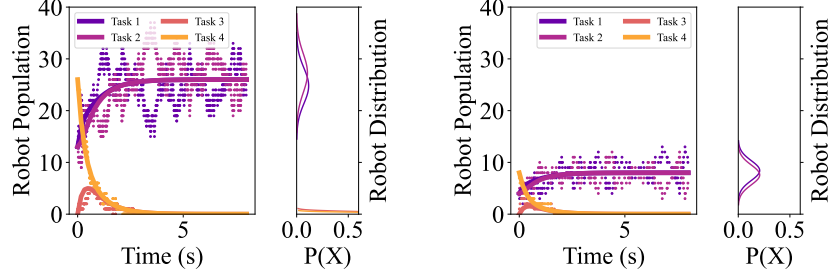
	$\beta_i = 0$ for $i = 1, \dots, 4$			$\beta_i \neq 0$ for $i = 1, \dots, 4$		
	$N = 52$	$N = 26$	$N = 16$	$N = 52$	$N = 26$	$N = 16$
$E[\mathbf{X}_1]$	24.8	12.8	8.2	25.2	13.3	7.5
$E[\mathbf{X}_2]$	26.5	12.7	7.7	25.6	14.6	8.3
$E[\mathbf{X}_3]$	0.5	0.0	0.0	0.6	0.0	0.1
$E[\mathbf{X}_4]$	0.2	0.0	0.0	0.4	0.0	0.0
$RV(\mathbf{X}_1)$	0.49	0.62	0.61	0.21	0.36	0.53
$RV(\mathbf{X}_2)$	0.54	0.63	0.69	0.21	0.23	0.47
$RV(\mathbf{X}_3)$	0.97	0.1	0.0	0.88	0.00	1.56
$RV(\mathbf{X}_4)$	0.75	0.1	0.0	1.38	0.00	0.00

Table 1: Expectation and Relative Variance (RV) of a series of numerical experiments considering different team sizes, with task graph in Figure 1 (a), initial and desired final distributions  $\mathbf{X}_0 = [25\% \ 25\% \ 0\% \ 50\%]'$ , and  $E[\mathbf{X}^d] = [50\% \ 50\% \ 0\% \ 0\%]'$ , respectively, and when  $\beta_i$  parameters are considered their values are given by  $\beta_1 = 0.05$ ,  $\beta_2 = 0.20$ ,  $\beta_3 = 0.11$ , and  $\beta_4 = 0.052$ .

robot system without  $\beta_i$  and with 52 robots is similar to the RV of a team with only 16 robots and  $\beta_i$  values. This suggests that our methodology improves the accuracy of the allocation of relatively small teams. Figures 2 (a) and (b) provide a realization for an instance with  $\beta_i = 0$  and  $N = 52$  and with  $\beta_i \neq 0$  and  $N = 16$ .

## 4.2 Experimental Results

Experimental tests were performed in the multi-robot Coherent Structure Testbed (mCoSTe). Figure 3 depicts the miniature autonomous surface vehicles (mASV) in Figure 3 (b), and the Multi-Robot Tank (MR tank) in Figure 3 (a). The MR Tank is a  $4.5\text{m} \times 3.0\text{m} \times 1.2\text{m}$  water tank equipped with an OptiTrack motion capture system. The mASVs are a differential drive platform, localized using 120 Hz motion capture data, communication link via XBee, and onboard processing with an Arduino Fio. Experiments were run for 4 minutes each, with  $\mathbf{X}_0 = [4 \ 0 \ 0 \ 0]'$ , and  $E[\mathbf{X}^d] = [1 \ 1 \ 1 \ 1]'$ , following the task graph outlined in Figure 1 (a). The parameters used for experimental trials were  $k_{ij} = 0.01$  for each nonzero and out-of-diagonal element of the matrix  $\mathbf{K}$ , and when variance control was used it was all  $\beta_i = 0.005$  for  $i = 1, \dots, 4$ . Those parameters were chosen to take into consideration the time necessary for the mASVs to travel among tasks. The parameters were converted to individual robot transitions by computing the likelihood of transition using equations (3) and (4), as well as which task the robot should transition to. At each task the mASVs were required to circle the location with a radius of 0.25m until a new transition was required.



(a) Realization without  $\beta_i$  and  $N = 52$       (b) Realization with  $\beta_i$  and  $N = 16$

Fig. 2: In (b) and (c) it is shown a realization of each of the stochastic simulations with  $N = 52$  and  $N = 16$ , respectively, where the dots represent the number of agents and the solid lines represent the numerical solution of (6). The figure axis are the same to help the visualization of the relative spread. The tasks are identified by the color caption and the graph topology is depicted in Figure 1 (a). The realization in (b) uses  $\beta_i = 0$ ,  $\forall i \in \mathcal{V}$ , while in (c) is with  $\beta_1 = 0.05$ ,  $\beta_2 = 0.20$ ,  $\beta_3 = 0.11$ , and  $\beta_4 = 0.052$ .

An instance of an experimental trial for both, with and without  $\beta_i$ , are included in Figure 4. The trajectory of each robot is represented by colors, the intensity of the colors is associated with its time occurrence—when the color is lighter that path was traveled by the respective mASV earlier in the experimental trial. Figure 4 (a) has a total of 28 transitions among tasks, those transitions take place throughout the experiment as indicated by darker lines between tasks. In the case of variance control, Figure 4 (b), there are 13 transitions among tasks, notice that many of these transitions happened earlier in the experiment. From five experimental trials without variance control the average number of task switches was 25.4, and from five experimental trials with variance control the average number of task switches was 15.6. This confirms that in the case where feedback is provided there is a reduced number of switches. A video illustrating our results can be found at <https://youtu.be/fTsX-5z6BUw>.

During experimentation we observed that sometimes the mASVs would transition before it could physically reach the assigned task, traveling diagonally among tasks. This was the case in Figure 4 (b) where Robot 4 quickly switched to another task while in transit. While this did not impact the overall results, it is an area of open interest to achieve desired parameters which leads to the desired task distribution within the capability of the robots.

## 5 Discussion

In the preceding sections, we have investigated the problem of stochastic allocation of multi-robot teams. For our main result, we formally demonstrated that



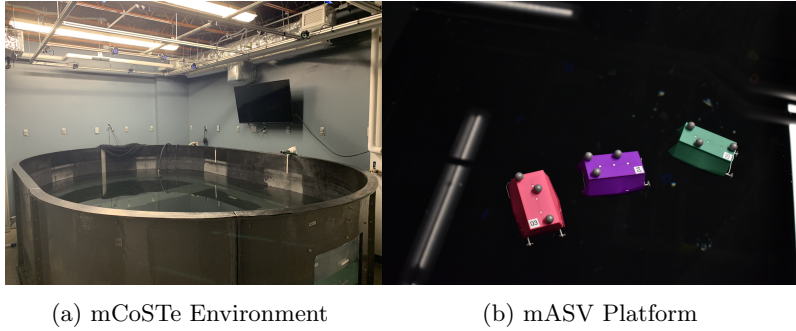


Fig. 3: The mCoSTe environment and mASV platform used for experimental results.

through a particular structure for the transition rates of the stochastic jump process model, we can decouple the first-order moments from the second-order moments. Such a decoupling allows us to introduce additional tuning variables to regulate the variance of the desired distribution of robots over tasks. The additional degree of freedom helps to reduce the impact of individual robots on the overall team’s performance. Therefore, the result of this contribution is to expand the viability of top-down stochastic models to include reduced-size robot teams. In general, the intuition for these models is that they are more accurate as the team size increases. However, when using our proposed method and directly adjusting the team variance it is possible to increase the top-down stochastic model accuracy for smaller teams. We argue that such refinement is a stride towards sparse swarms—even though we are technically approaching the team size problem and ignoring the task space size.

Although we have formally shown the impact of the additional tuning variables as well as the decoupling between first- and second-order moments, and also experimentally and numerically investigated the influence of such variables, we did not draw general mathematical expressions to compute their values during the design stage. In our investigations, we used a greedy algorithm that increased the variable number based on the desired values of variance and final distribution. In addition, our optimization problem to compute the gain matrix  $\mathbf{K}$  for a desired distribution incorporates designer knowledge about the robot capabilities through the set  $\mathcal{K}$ , which will directly affect the robots’ mean transition time. We plan to formalize this unsolved concern in future investigations.

## 6 Conclusions and future work

We have provided a new structure for the transition rates for ensemble robot distributions modeled from a top-down perspective. As a first result, we have demonstrated that such a structure leads to uncoupled parameters to adjust the mean and the variance of desired team’s distribution. Then, based on this

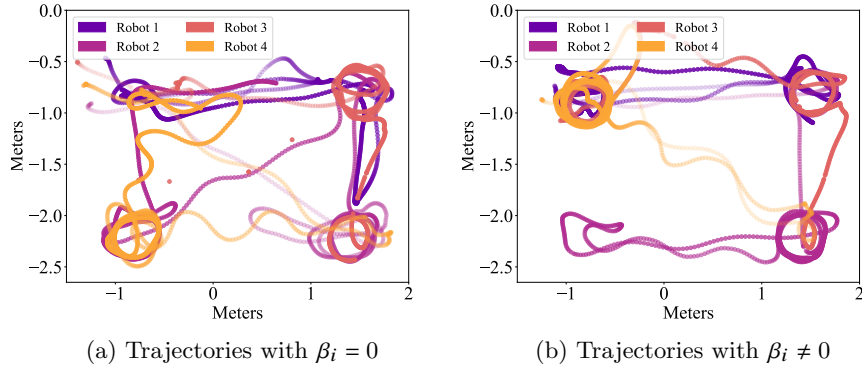


Fig. 4: Experimental results from a 4 minute and 4 mASV run, with task graph in Figure 1 (a). The desired distribution is one agent at each task. The test in Figure 4 (a) had 28 switches, while in Figure 4 (b) it had 13 switches. The colors' intensity reflects time—the lighter the color the earlier that path was cruised in the trial.

finding, we examined simple design strategies to compute the necessary gains. This approach provides an efficient ensemble behavior for relatively small groups. Finally, physical and numerical experiments were implemented, illustrating the effectiveness of the method. Possible future work includes the extension of the strategy for distributed regulation. A potential strategy is to perform distributed estimates of the number of agents performing each task. It is also of interest to connect the robot dynamics with the changing transition rates. One possible approach to bridging those two models is through hybrid switching systems. A formal methodology to design the network structure for a given covariance bound will be considered in the future.

## Acknowledgements

We gratefully acknowledge the support of ARL DCIST CRA W911NF-17-2-0181, Office of Naval Research (ONR) Award No. N00014-22-1-2157, and the National Defense Science & Engineering Graduate (NDSEG) Fellowship Program.

## References

1. Berman, S., Halász, A., Hsieh, M.A., Kumar, V.: Optimized stochastic policies for task allocation in swarms of robots. *IEEE transactions on robotics* **25**(4), 927–937 (2009)
2. Deshmukh, V., Elamvazhuthi, K., Biswal, S., Kakish, Z., Berman, S.: Mean-field stabilization of markov chain models for robotic swarms: Computational approaches and experimental results. *IEEE Robotics and Automation Letters* **3**(3), 1985–1992 (2018). DOI 10.1109/LRA.2018.2792696

3. Elamvazhuthi, K., Berman, S.: Mean-field models in swarm robotics: a survey. *Bioinspiration & Biomimetics* **15**(1), 015001 (2019). DOI 10.1088/1748-3190/ab49a4
4. Elamvazhuthi, K., Biswal, S., Berman, S.: Controllability and decentralized stabilization of the kolmogorov forward equation for markov chains. *Automatica* **124**, 109351 (2021). DOI <https://doi.org/10.1016/j.automatica.2020.109351>
5. Gerkey, B.P., Mataric, M.J.: A formal analysis and taxonomy of task allocation in multi-robot systems. *The International journal of robotics research* **23**(9), 939–954 (2004)
6. Gillespie, D.T.: Exact stochastic simulation of coupled chemical reactions. *The journal of physical chemistry* **81**(25), 2340–2361 (1977)
7. Hamann, H.: Towards swarm calculus: Universal properties of swarm performance and collective decisions. In: M. Dorigo, M. Birattari, C. Blum, A.L. Christensen, A.P. Engelbrecht, R. Groß, T. Stützle (eds.) *Swarm Intelligence*, pp. 168–179. Springer Berlin Heidelberg, Berlin, Heidelberg (2012)
8. Hsieh, M.A., Halász, Á., Berman, S., Kumar, V.: Biologically inspired redistribution of a swarm of robots among multiple sites. *Swarm Intelligence* **2**(2), 121–141 (2008)
9. Khalil, H.K.: *Nonlinear Systems*, vol. 10, third edn. Prentice Hall (2002)
10. Klavins, E.: Proportional-integral control of stochastic gene regulatory networks. In: 49th IEEE Conference on Decision and Control (CDC), pp. 2547–2553. IEEE (2010)
11. Mather, T.W., Hsieh, M.A.: Distributed robot ensemble control for deployment to multiple sites. In: *Robotics: Science and Systems VII* (2011)
12. Mather, T.W., Hsieh, M.A.: Ensemble modeling and control for congestion management in automated warehouses. In: 2012 IEEE International Conference on Automation Science and Engineering (CASE), pp. 390–395 (2012). DOI 10.1109/CoASE.2012.6386498
13. Nam, C., Shell, D.A.: When to do your own thing: Analysis of cost uncertainties in multi-robot task allocation at run-time. In: 2015 IEEE International Conference on Robotics and Automation (ICRA), pp. 1249–1254 (2015). DOI 10.1109/ICRA.2015.7139351
14. Nam, C., Shell, D.A.: Analyzing the sensitivity of the optimal assignment in probabilistic multi-robot task allocation. *IEEE Robotics and Automation Letters* **2**(1), 193–200 (2017). DOI 10.1109/LRA.2016.2588138
15. Napp, N., Burden, S., Klavins, E.: Setpoint regulation for stochastically interacting robots. *Autonomous Robots* **30**(1), 57–71 (2011). DOI 10.1007/s10514-010-9203-2
16. Øksendal, B., Sulem, A.: *Applied Stochastic Control of Jump Diffusions*, 2 edn. Springer Berlin Heidelberg, Berlin, Heidelberg (2007). DOI 10.1007/978-3-540-69826-5
17. Prorok, A., Hsieh, M.A., Kumar, V.: The impact of diversity on optimal control policies for heterogeneous robot swarms. *IEEE Transactions on Robotics* **33**(2), 346–358 (2017)
18. Ravichandar, H., Shaw, K., Chernova, S.: Strata: unified framework for task assignments in large teams of heterogeneous agents. *Auton. Agents Multi Agent Syst.* **34**(2), 38 (2020)
19. Tarapore, D., Groß, R., Zauner, K.P.: Sparse robot swarms: Moving swarms to real-world applications. *Frontiers in Robotics and AI* **7** (2020). DOI 10.3389/frobt.2020.00083